

See discussions, stats, and author profiles for this publication at: <https://www.researchgate.net/publication/236206787>

# Facile Encapsulation of Oxide based Thin Film Transistors by Atomic Layer Deposition based on Ozone

ARTICLE *in* ADVANCED MATERIALS · MAY 2013

Impact Factor: 17.49 · DOI: 10.1002/adma.201300549 · Source: PubMed

CITATIONS

10

READS

43

6 AUTHORS, INCLUDING:



**Morteza Fakhri**

Bergische Universität Wuppertal

9 PUBLICATIONS 54 CITATIONS

SEE PROFILE



**Andreas Behrendt**

Bergische Universität Wuppertal

19 PUBLICATIONS 266 CITATIONS

SEE PROFILE



**Patrick Görrn**

Bergische Universität Wuppertal

53 PUBLICATIONS 1,140 CITATIONS

SEE PROFILE



**Thomas Riedl**

Bergische Universität Wuppertal

151 PUBLICATIONS 4,123 CITATIONS

SEE PROFILE

# Facile Encapsulation of Oxide based Thin Film Transistors by Atomic Layer Deposition based on Ozone

Morteza Fakhri, Nikolai Babin, Andreas Behrendt, Timo Jakob, Patrick Görrn, and Thomas Riedl\*

Thin film transistors (TFT) based on transparent amorphous oxide semiconductors (TAOS) have been the object of tremendous interest during the past few years.<sup>[1–3]</sup> TFTs based on TAOS channel semiconductors have been evidenced to show a high carrier mobility even in the amorphous phase.<sup>[4,5]</sup> Therefore, applications like high performance pixel driver electronics for high resolution displays and large-area flexible electronic systems are envisaged.<sup>[6,7]</sup> Commonly, metal-oxide based TFTs are sensitive towards ambient gases like oxygen and water.<sup>[8,9]</sup> The adsorption of oxygen at the channel surface crucially affects the TFT characteristics.<sup>[10–12]</sup> Similarly, the transfer characteristics as well as the hysteresis of TFTs are influenced by adsorbed water.<sup>[13,14]</sup> At the same time, the degradation of device parameters under illumination and bias stress is accelerated in the presence of ambient gases.<sup>[15]</sup> Therefore, a proper encapsulation of the metal-oxide based TFT is mandatory in order to reduce the influence of ambient gases and to achieve stable devices. Common techniques for the preparation of gas diffusion barrier layers are chemical vapor deposition (CVD), sputtering and atomic layer deposition (ALD).<sup>[16–19]</sup> Among them, ALD has been shown to yield barrier layers with outstandingly low permeation rates for water and oxygen.<sup>[20,21]</sup> However, encapsulation of metal-oxide TFTs with conventional ALD using water as oxygen source is found to substantially alter device characteristics, most prominently the threshold voltage.<sup>[19]</sup> Post-annealing of the devices in oxidizing atmosphere is often necessary to recover the original transistor properties. This requirement for post processing is time and energy consuming and adds substantially to production complexity and cost.

In this report, we demonstrate a facile encapsulation approach for metal-oxide based TFTs using ozone as the oxidizing agent in an ALD process. In stark contrast to the established water-based ALD processes, ozone as in-situ source for oxygen prevents the shift of threshold voltage during the deposition of the encapsulation layer. Thus, no post-deposition annealing of the encapsulated TFT in oxygen atmosphere is required to restore its characteristics before encapsulation. Moreover, the hysteresis present in un-encapsulated transistors can be permanently suppressed by the ALD encapsulation. It is

especially important to stress, that we are able to show that this approach is of general validity for various ALD encapsulation materials (e.g.  $\text{Al}_2\text{O}_3$ ,  $\text{TiO}_x$ ,  $\text{ZrO}_2$ ) and applies to several important metal oxide channel semiconductors, like zinc-tin-oxide (ZTO) and indium-gallium-zinc-oxide (IGZO).

A typical transfer characteristic of a ZTO transistor (channel thickness: 50 nm) before (square symbols) and after (circle symbols) ALD encapsulation using a conventional TMA and water process is illustrated in **Figure 1**. The threshold voltage ( $V_{th}$ ) of the device is severely reduced upon encapsulation by more than 25 V from 3.1 V down to -23 V. Opposed to that, the saturation mobility  $\mu_{sat} \approx 7 \text{ cm}^2(\text{Vs})^{-1}$  remains unaffected. In previous reports, the reduction of  $V_{th}$  in a similar ALD process has been related to the removal of oxygen during the process.<sup>[22]</sup> TMA and other metal-organic ALD precursors are known to be strong Lewis acids. The oxygen molecule itself is also a Lewis acid, and it is well known that TMA does not chemically react with neutral  $\text{O}_2$ .<sup>[23]</sup> On the other hand, negatively charged oxygen at the surface of a metal oxide is substantially less Lewis acidic and has even been classified as Lewis base.<sup>[24,25]</sup> As a result, a chemical reaction of the Lewis acid TMA with the negatively charged oxygen becomes possible. A detailed discussion of the interaction of a Lewis acid-base pair on oxide surfaces has been reported elsewhere.<sup>[24,25]</sup>

With regard to the TFT, adsorbed oxygen at the surface of a metal oxide channel leads to a negative surface charge and a depletion layer due to trapping of electrons from the semiconductor channel.<sup>[11]</sup> Detrapping of electrons after removal of these oxygen related states leads to an increase of free charge carrier density in the TFT channel and consequently to a lowered threshold voltage.<sup>[18,22]</sup> This effect has been generally observed for other transistors with a TAOS channel, like those based on IGZO.<sup>[19]</sup> Commonly, a post-treatment step like annealing of the encapsulated TFT in oxidizing atmosphere is, therefore, necessary in order to re-establish the adsorbed oxygen at the TFT channel and thereby to reduce the free charge carrier density and recover the original device characteristics. As an example, Figure 1 (triangular symbols) includes the transfer characteristics of the encapsulated TFT after annealing at 200 °C for 10 min in air. The original value of the threshold voltage ( $V_{th} = 3.1 \text{ V}$ ) before encapsulation is almost fully recovered by this annealing step. Obviously, annealing in air leads to re-adsorption of oxygen, as a result of the thermally activated increase of gas permeability of the  $\text{Al}_2\text{O}_3$  barrier at elevated temperatures.<sup>[20]</sup> Interestingly, the hysteresis is significantly reduced due to the encapsulation compared to the initial value. This effect can be accounted to the desorption of water during the encapsulation process in vacuum. Recent studies

M. Fakhri, N. Babin, A. Behrendt, T. Jakob,  
Prof. P. Görrn, Prof. T. Riedl  
University of Wuppertal  
Institute of Electronic Devices  
Rainer-Gruenter-Str. 21, 42119 Wuppertal, Germany  
E-mail: t.riedl@uni-wuppertal.de



DOI: 10.1002/adma.201300549

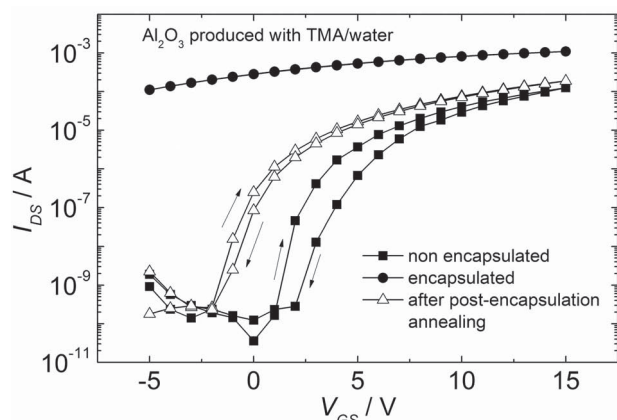


**Figure 1.** Transfer characteristics of encapsulated TFTs using ALD with water as oxidizing agent: device characteristics before encapsulation (squares), after encapsulation (circles), after post-encapsulation annealing at 200 °C for 10 min in air (triangles).

have already demonstrated the impact of water on the hysteresis of ZTO TFTs.<sup>[14,26]</sup>

From an application point of view, it would be extremely desirable to avoid the requirement for any costly energy- and time-consuming post-treatment process. We therefore demonstrate the encapsulation of metal-oxide based TFTs using ALD barriers prepared with ozone instead of water as oxidizing agent. We will show that, thereby, we can overcome the requirement for any post-encapsulation treatment. In general, ALD processes based on ozone are well established and the ALD reaction scheme of the TMA and O<sub>3</sub> process has been clarified before, e.g. ref.[27]. However, as of yet, ALD barrier layers based on ozone have not yet been used for the encapsulation of metal-oxide TFTs. **Figure 2** illustrates the transfer characteristics of a TFT before (square symbols) and after (circle symbols) the encapsulation with a TMA/O<sub>3</sub> process. In contrast to the device that is encapsulated using water, the threshold voltage is only negligibly shifted from 2.7 V to 1.3 V upon encapsulation. As opposed to the TMA/H<sub>2</sub>O process the in-situ supply of oxygen

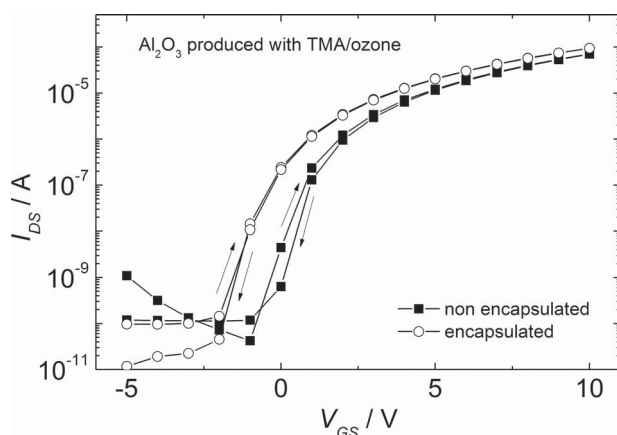


**Figure 2.** Transfer characteristics of encapsulated TFTs using ALD with ozone as oxidizing agent: characteristics before encapsulation (squares) and after encapsulation (circles).

in the TMA/O<sub>3</sub> process allows for re-adsorption of oxygen at the TFT channel surface and thereby a threshold voltage similar to that of the TFT before encapsulation is preserved. It is worth to note, that the mobility,  $\mu_{\text{sat}} = 8 \text{ cm}^2(\text{Vs})^{-1}$ , is almost unaffected while the hysteresis of the encapsulated TFT is almost entirely eliminated. A detailed summary of the TFT properties before and after encapsulation using TMA/O<sub>3</sub> is given in the supporting information (Table S1).

To study the effect of ozone in this process, the TFT has been in-situ characterized during the first cycles of the ALD encapsulation process. It is essential to note beforehand, that the ozone treatment of TFTs without encapsulation leaves their device characteristics unchanged.

**Figure 3(a)** illustrates the threshold voltage  $V_{\text{th}}$  of the TFT upon TMA ( $t_{\text{pulse}} = 200 \text{ ms}$ ) and ozone exposure. As expected,  $V_{\text{th}}$  is strongly reduced upon exposure to a single TMA pulse. However, the threshold voltage fully recovers after introducing ozone into the reactor. Notably, the time constant of this process ( $\tau$ ) is smaller than the time resolution ( $\Delta t$ ) of the experiment ( $\tau \ll \Delta t = 1 \text{ min}$ ). Obviously, ozone leads to a fast adsorption of oxygen at the semiconductor surface, which consequently increases  $V_{\text{th}}$  towards the original value. Strikingly, a similarly fast re-adsorption of oxygen cannot be achieved if the device is exposed to O<sub>2</sub> instead of ozone. **Figure 3(b)** depicts  $V_{\text{th}}$  as a

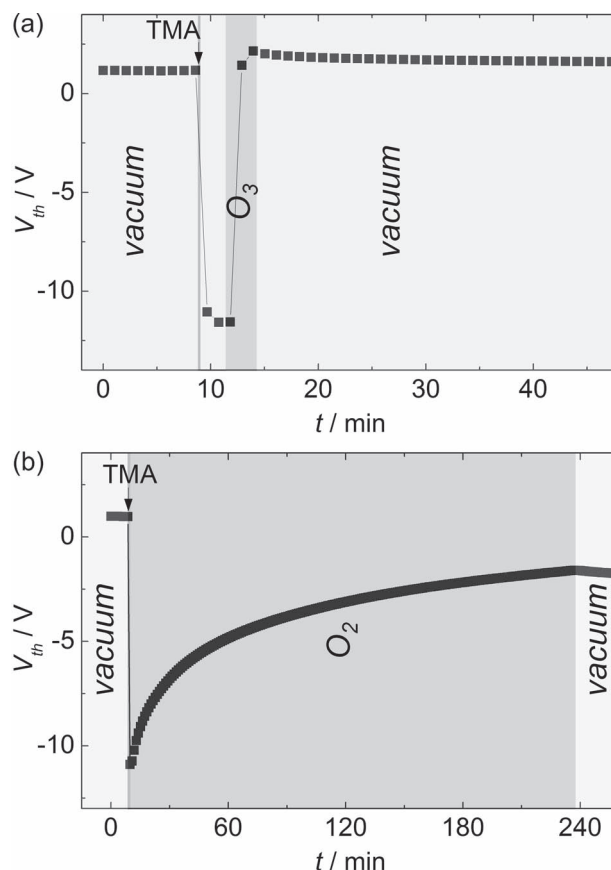


**Figure 3.** Time dependence of  $V_{\text{th}}$  upon TMA exposure ( $t_{\text{pulse}} = 200 \text{ ms}$ ) and subsequent O<sub>3</sub> exposure ( $t_{\text{O}_3} = 2 \text{ min}$ ) (a), or subsequent O<sub>2</sub> exposure (b), respectively.

function of time upon  $O_2$  exposure. The adsorption of oxygen due to  $O_2$  exposure ( $p_{O_2} = 2$  mbar) reveals a time constant ( $\tau = 1.7$  h) several orders of magnitude larger than that seen upon  $O_3$  exposure ( $\tau \ll 1$  min). This difference in adsorption time constant can be explained by the higher electron affinity of ozone compared to that of  $O_2$ <sup>[28]</sup> which is expected to lead to a more efficient capture of an electron from the semiconductor channel.

In the following we have studied the in-situ diffusion processes during an encapsulation process based on both water and ozone. We first designed an experiment to obtain an estimate for a barrier thickness of  $Al_2O_3$  that is sufficient to hinder TMA diffusion to the TFT channel surface. To this end, we study a bi-layered barrier as shown in the inset of Figure 4(a). Specifically, the overall  $Al_2O_3$  encapsulation layer has a thickness of  $d = 50$  nm and is composed of an  $Al_2O_3$  layer prepared from TMA/ozone (thickness  $d_{O_3}$ ) and a subsequently deposited  $Al_2O_3$  layer prepared from TMA/water (thickness  $d_{H_2O}$ ). Figure 4(a) depicts the change of the threshold voltage  $\Delta V_{th}$  upon encapsulation in dependence on the film thickness  $d_{O_3}$ . As discussed, a barrier layer prepared only from TMA/water ( $d_{O_3} =$

0 nm) leads to a strong negative shift of the threshold voltage by about 20 V. On the contrary, using only a 1 nm thick  $Al_2O_3$  interlayer produced with TMA/ozone already substantially reduces the threshold voltage shift to only  $\Delta V_{th} = -2.5$  V. An increase of the interlayer thickness ( $d_{O_3}$ ) shows no substantial further effect. These results tell us, that already a 1 nm thin  $Al_2O_3$  barrier prepared by TMA/ozone is able to protect the TFT channel against precursors used in a subsequent ALD process. This would be relevant for a subsequent ALD process in which ozone does not work as oxidizing agent. Our results of this experiment also show that the severe shift of the threshold voltage as seen in a TMA/water ALD process already happens within the first nanometer of deposition. Importantly, the data presented in Figure 4 (a) also tells us, that potentially trapped charges in the deeper volume of the encapsulation layer prepared from TMA/water do not significantly affect  $V_{th}$ , as in the presence of the 1 nm thin  $Al_2O_3$  barrier (TMA/ozone)  $\Delta V_{th}$  is independent of the thickness  $d_{H_2O}$ . In a similar sense, as  $\Delta V_{th}$  is independent of the distance ( $d_{O_3} \geq 1$  nm) of the extra interface within the bi-layer from the TFT channel, we can rule out a significant contribution of trapped charges at this interface.

In an analogy to the experiment above, the sequence of the TMA/water and TMA/ozone layers is now flipped. From this set of samples, we intend to learn if the ozone used in the TMA/ozone process can diffuse through the already existing  $Al_2O_3$  layer. As above, the TFT is encapsulated by a bi-layer, this time starting with TMA/water (thickness  $d_{H_2O}$ ) and a subsequent  $Al_2O_3$  layer made with TMA/ozone (thickness  $d_{O_3}$ ) (see inset of Figure 4 (b)). Again, the overall barrier thickness is kept constant ( $d = d_{O_3} + d_{H_2O} = 50$  nm). Figure 4 (b) illustrates the change of the threshold voltage  $\Delta V_{th}$  upon variation of  $d_{H_2O}$ . While  $\Delta V_{th}$  is almost zero for  $d_{H_2O} < 5$  nm, a steady decrease of  $\Delta V_{th}$  can be observed for  $d_{H_2O} > 5$  nm. In case of a barrier layer produced with TMA/water only (this means  $d_{H_2O} = 50$  nm), the threshold voltage is strongly shifted to -20 V, as discussed before. These results demonstrate that ozone can diffuse through an already existing (thin)  $Al_2O_3$  layer. It can supply oxygen to the TFT surface and consequently recover the threshold voltage of the TFT before encapsulation. The possibility to recover the threshold is more and more limited with increasing thickness  $d_{H_2O}$  of the already existing  $Al_2O_3$  layer due to hampered diffusion of ozone to the TFT channel surface. This experiment clearly supports our above conclusion, that ozone really is responsible for the recovery of the initial TFT characteristics by the re-establishment of negatively charged oxygen at the TFT channel surface. Obviously, a similar mechanism is not possible for  $H_2O$ .

It is important to note, that our finding has a general character and applies for encapsulation layers other than  $Al_2O_3$  and other metal-oxide channel semiconductors. Table 1 summarizes the shift of the threshold voltage  $\Delta V_{th}$  and the reduction of the hysteresis  $V_h$  upon encapsulation with  $Al_2O_3$ ,  $TiO_2$  and  $ZrO_2$ . If IGZO is used as channel material instead of ZTO, a shift of threshold voltage is also found upon encapsulation using an ALD process based on water. We want to note that the shift of  $V_{th}$  upon encapsulation is smaller than found for the ZTO devices. This may be attributed to different preparation conditions of the ZTO and IGZO channel semiconductor. The MF sputter deposition used for IGZO may lead to a substantially reduced density of negatively charged chemisorbed oxygen

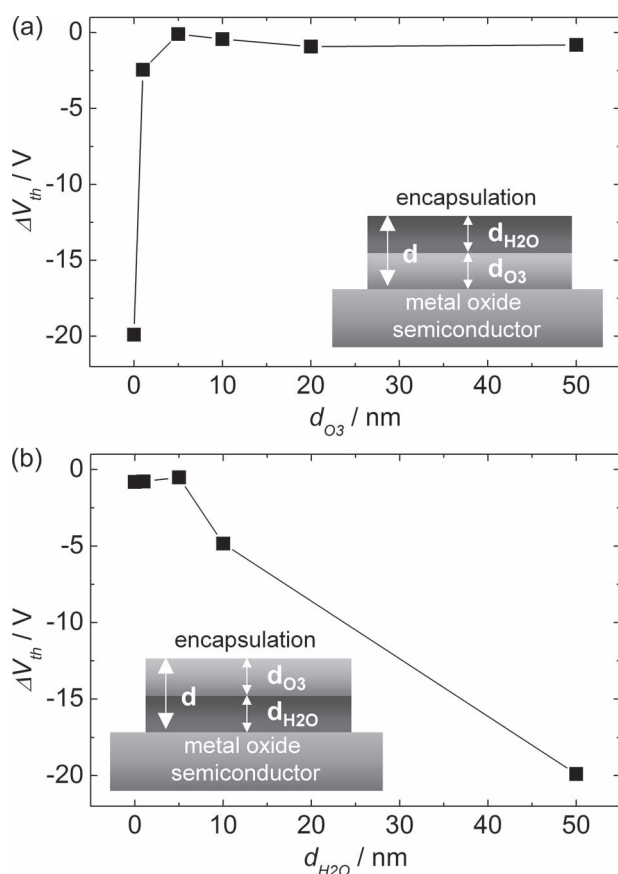


**Figure 4.** Change of the threshold voltage  $\Delta V_{th}$  upon encapsulation with a bi-layered barrier.  $d_{O_3}$ ,  $d_{H_2O}$  represent the thickness of the  $Al_2O_3$  layer produced with ozone and water as oxidant agent, respectively. The overall  $Al_2O_3$  layer thickness is kept at  $d = d_{O_3} + d_{H_2O} = 50$  nm. (a) Barrier layer using first ozone and then water as oxidizing agents. (b) Encapsulation by flipping the layer sequence and using first water and then ozone as oxidizing agent.

**Table 1.** Shift of threshold voltage  $\Delta V_{th}$  and reduction of hysteresis  $\Delta V_h$  (with reference to the initial hysteresis voltage before encapsulation  $V_{h,0}$ ) upon encapsulation with various dielectrics using water or ozone as oxidizing agent. Note, that  $V_h$  can only be determined for devices encapsulated using ozone, where a reasonable transfer characteristic is detected.

Encapsulation material	Channel material	$\Delta V_{th}$ [V]		$\Delta V_h/V_{h,0}$ ozone
		water	ozone	
$Al_2O_3$	–	–20	–1.4	–70%
$TiO_2$	ZTO	–29.5	–1.8	–40%
$ZrO_2$	ZTO	–9	–1.4	–100%
$Al_2O_3$	IGZO	–1.1	0.1	–50%

than in the case of the RF sputtered ZTO channels. Nevertheless, as reported for ZTO, the shift of  $V_{th}$  in the IGZO TFTs can be entirely avoided when they are encapsulated using TMA and ozone instead of TMA and water.

Finally, we have investigated the long-term behavior of our ALD encapsulated devices based on ozone. For this purpose, we have measured the transistors over a time period of about 40 days. **Figure 5** shows the threshold voltage  $V_{th}$  and the hysteresis  $V_h$  vs. time. The first data point denotes the TFT characteristics before encapsulation, while the further data points are measured after encapsulation and storage in a dark air ambient at room temperature. The outstanding stability of  $V_{th}$  and the small residual hysteresis of only 80 mV, reflects the excellent barrier characteristics of the  $Al_2O_3$  encapsulation layer prepared with TMA and ozone against the penetration of oxygen and moisture. This finding is of particular importance for a stable operation of metal oxide based TFTs unaffected by ambient gases.

In conclusion, we have shown that the encapsulation of TFTs based on a metal-oxide semiconductor with a metal-oxide gas diffusion barrier using conventional atomic layer deposition (ALD) with water as oxygen source is found to substantially alter device characteristics. Specifically, a strong reduction of the threshold voltage is encountered, as a result of the reaction

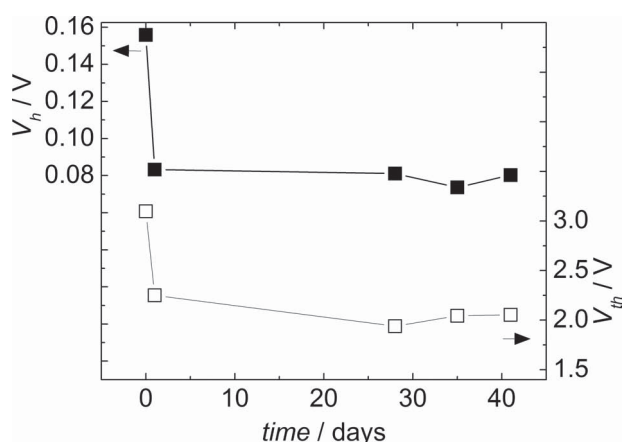


**Figure 5.** Long-term behavior of the threshold voltage  $V_{th}$  and hysteresis  $V_h$  of devices encapsulated with 50 nm of  $Al_2O_3$  (prepared with TMA/ozone) vs. time. First data point indicates device characteristics before encapsulation.

of the Lewis-acidic metal-organic precursors with negatively charged chemisorbed oxygen. Therefore, post-annealing in oxidizing atmosphere is typically required to partly recover the original TFT characteristics. To overcome this issue, we have demonstrated a simplified encapsulation, using ozone instead of water as an oxygen source in a low-temperature ALD process, which leaves the threshold voltage unaltered and the hysteresis permanently reduced. Thereby, any costly energy- and time-consuming post-treatment processes can be avoided. Remarkably, this concept is widely applicable to various encapsulation materials (e.g.  $Al_2O_3$ ,  $TiO_2$ ,  $ZrO_2$ ) and metal-oxide channel semiconductors (e.g. zinc-tin-oxide (ZTO), indium-gallium-zinc-oxide (IGZO)).

## Experimental Section

The staggered bottom gate TFTs in this study are fabricated on glass substrates coated with a 200 nm indium tin oxide (ITO) gate electrode and a 220 nm thick dielectric composed of  $Al_2O_3$  and  $TiO_2$  multilayers, prepared by atomic layer deposition. The ZTO channel layer has been deposited by RF-magnetron sputtering at room temperature. A detailed preparation procedure is given in ref. [29]. The IGZO TFTs were fabricated by depositing the channel layer with MF-magnetron sputtering at room temperature in a mixed sputtering atmosphere of argon and oxygen ( $p_{O_2} = 3\%$ ). All devices were post-annealed at 400 °C. Finally, the TFTs are encapsulated with a 50 nm thick  $Al_2O_3$  layer, produced by ALD with water or ozone as oxidizing agent at 80 °C (in a Beneq TFS 200 ALD system). As metal-organic precursors we used trimethylaluminum (TMA) for  $Al_2O_3$ , titaniumisopropoxid for  $TiO_2$ , and tetrakis(dimethylamido)zirconium(IV) for  $ZrO_2$ . All experiments have been done in darkness, to avoid effects of illumination on the device characteristics [30].

## Supporting Information

Supporting Information is available from the Wiley Online Library or from the author.

## Acknowledgements

P.G. acknowledges funding by the Emmy-Noether-Programm of the DFG (Deutsche Forschungsgemeinschaft).

Received: February 1, 2013  
Published online: April 17, 2013

- [1] R. L. Hoffman, B. J. Norris, J. F. Wager, *Appl. Phys. Lett.* **2003**, 82, 733.
- [2] K. Nomura, H. Ohta, A. Takagi, T. Kamiya, M. Hirano, H. Hosono, *Nature* **2004**, 432, 488–92.
- [3] E. Fortunato, P. Barquinha, R. Martins, *Adv. Mater.* **2012**, 24, 2945–2986.
- [4] J. K. Jeong, J. H. Jeong, H. W. Yang, J.-S. Park, Y.-G. Mo, H. D. Kim, *Appl. Phys. Lett.* **2007**, 91, 113505.
- [5] H. Q. Chiang, J. F. Wager, R. L. Hoffman, J. Jeong, D. a. Keszler, *Appl. Phys. Lett.* **2005**, 86, 013503.
- [6] P. Görrn, F. Ghaffari, T. Riedl, W. Kowalsky, *Solid-State Electron.* **2009**, 53, 329–331.
- [7] P. Görrn, M. Sander, J. Meyer, M. Kröger, E. Becker, H.-H. Johannes, W. Kowalsky, T. Riedl, *Adv. Mater.* **2006**, 18, 738–741.



- [8] D. Kang, H. Lim, C. Kim, I. Song, J. Park, Y. Park, J. Chung, *Appl. Phys. Lett.* **2007**, *90*, 192101.
- [9] J.-S. Park, J. K. Jeong, H.-J. Chung, Y.-G. Mo, H. D. Kim, *Appl. Phys. Lett.* **2008**, *92*, 072104.
- [10] E. Chong, Y. S. Chun, S. H. Kim, S. Y. Lee, *J. Electrical Engineering & Technology* **2011**, *6*, 539–542.
- [11] P.-T. Liu, Y.-T. Chou, L.-F. Teng, *Appl. Phys. Lett.* **2009**, *95*, 233504.
- [12] J. K. Jeong, H. Won Yang, J. H. Jeong, Y.-G. Mo, H. D. Kim, *Appl. Phys. Lett.* **2008**, *93*, 123508.
- [13] S. Yang, C.-S. Hwang, J.-I. Lee, S.-M. Yoon, M.-K. Ryu, K.-I. Cho, S.-H. K. Park, S.-H. Kim, C.-E. Park, J. Jang, *Appl. Phys. Lett.* **2011**, *98*, 103515.
- [14] M. Fakhri, H. Johann, P. Görrn, T. Riedl, *ACS Appl. Mater. Interfaces* **2012**, *4*, 4453.
- [15] K.-H. Lee, J. S. Jung, K. S. Son, J. S. Park, T. S. Kim, R. Choi, J. K. Jeong, J.-Y. Kwon, B. Koo, S. Lee, *Appl. Phys. Lett.* **2009**, *95*, 232106.
- [16] J.-M. Lee, I.-T. Cho, J.-H. Lee, H.-I. Kwon, *Appl. Phys. Lett.* **2008**, *93*, 093504.
- [17] J. Park, S. Kim, C. Kim, S. Kim, I. Song, H. Yin, K.-K. Kim, S. Lee, K. Hong, J. Lee, J. Jung, E. Lee, K.-W. Kwon, Y. Park, *Appl. Phys. Lett.* **2008**, *93*, 053505.
- [18] A. Olziersky, P. Barquinha, A. Vilà, L. Pereira, G. Gonçalves, E. Fortunato, R. Martins, J. R. Morante, *J. Appl. Phys.* **2010**, *108*, 064505.
- [19] D. H. Cho, S. H. Yang, J.-H. Shin, C. W. Byun, M. K. Ryu, J. I. Lee, C. S. Hwang, H. Y. Chu, *J. Korean Phys. Soc.* **2009**, *54*, 531.
- [20] J. Meyer, P. Görrn, F. Bertram, S. Hamwi, T. Winkler, H. Johannes, T. Weimann, P. Hinze, T. Riedl, W. Kowalsky, *Adv. Mater.* **2009**, *21*, 1845–1849.
- [21] J. Meyer, H. Schmidt, W. Kowalsky, T. Riedl, A. Kahn, *Appl. Phys. Lett.* **2010**, *96*, 243308.
- [22] P. Görrn, T. Riedl, W. Kowalsky, *J. Phys. Chem. C* **2009**, *113*, 11126–11130.
- [23] J. Koo, S. Kim, S. Jeon, H. Jeon, *J. Korean Phys. Soc.* **2006**, *48*, 131–136.
- [24] P. C. Stair, *J. Am. Chem. Soc.* **1982**, *104*, 4044–4052.
- [25] H. Metiu, S. Chretien, Z. Hu, B. Li, X. Sun, *J. Phys. Chem. C* **2012**, *116*, 10439–10450.
- [26] D. Kim, S. Yoon, Y. Jeong, Y. Kim, B. Kim, M. Hong, *Appl. Phys. Express* **2012**, *5*, 021101.
- [27] D. N. Goldstein, J. A. McCormick, S. M. George, *J. Phys. Chem. C* **2008**, *112*, 19530–19539.
- [28] M. D. Hernández-Alonso, J. M. Coronado, A. Javier Maira, J. Soria, V. Loddo, V. Augugliaro, *Appl. Catal., B* **2002**, *39*, 257–267.
- [29] M. Fakhri, P. Görrn, T. Weimann, P. Hinze, T. Riedl, *Appl. Phys. Lett.* **2011**, *99*, 123503.
- [30] P. Görrn, M. Lehnhardt, T. Riedl, W. Kowalsky, *Appl. Phys. Lett.* **2007**, *91*, 193504.